Behavioral/Cognitive

Asymmetric Frequency-Specific Feedforward and Feedback Information Flow between Hippocampus and Prefrontal Cortex during Verbal Memory Encoding and Recall

Anup Das[1]* **and Vinod Menon**[1,2,3]*

[1]Department of Psychiatry & Behavioral Sciences, [2]Department of Neurology & Neurological Sciences, and [3]Stanford Neurosciences Institute, Stanford University School of Medicine, Stanford, California 94305

Hippocampus and prefrontal cortex (PFC) circuits are thought to play a prominent role in human episodic memory, but the precise nature, and electrophysiological basis, of directed information flow between these regions and their role in verbal memory formation has remained elusive. Here we investigate nonlinear causal interactions between hippocampus and lateral PFC using intracranial EEG recordings (26 participants, 16 females) during verbal memory encoding and recall tasks. Direction-specific information theoretic analysis revealed higher causal information flow from the hippocampus to PFC than in the reverse direction. Crucially, this pattern was observed during both memory encoding and recall, and the strength of causal interactions was significantly greater during memory task performance than resting baseline. Further analyses revealed frequency specificity of interactions with greater causal information flow from hippocampus to the PFC in the delta-theta frequency band (0.5-8 Hz); in contrast, PFC to hippocampus causal information flow were stronger in the beta band (12-30 Hz). Across all hippocampus-PFC electrode pairs, propagation delay between the source and target signals was estimated to be 17.7 ms, which is physiologically meaningful and corresponds to directional signal interactions on a timescale consistent with monosynaptic influence. Our findings identify distinct asymmetric feedforward and feedback signaling mechanisms between the hippocampus and PFC and their dissociable roles in memory recall, demonstrate that these regions preferentially use different frequency channels, and provide novel insights into the electrophysiological basis of directed information flow during episodic memory formation in the human brain.

Key words: **hippocampus; human iEEG; information flow; phase transfer entropy and causal dynamics; prefrontal cortex; verbal memory encoding and recall**

Significance Statement

Hippocampal-PFC circuits play a critical role in episodic memory in rodents, nonhuman primates, and humans. Investigations using noninvasive fMRI techniques have provided insights into coactivation of the hippocampus and PFC during memory formation; however, the electrophysiological basis of dynamic causal hippocampal-PFC interactions in the human brain is poorly understood. Here, we use data from a large cohort of intracranial EEG recordings to investigate the neurophysiological underpinnings of asymmetric feedforward and feedback hippocampal-PFC interactions and their nonlinear causal dynamics during both episodic memory encoding and recall. Our findings provide novel insights into the electrophysiological basis of directed bottom-up and top-down information flow during episodic memory formation in the human brain.

Received Apr. 14, 2021; revised July 5, 2021; accepted July 21, 2021.

Author contributions: A.D. and V.M. designed research; A.D. and V.M. performed research; A.D. analyzed data; A.D. and V.M. wrote the first draft of the paper; A.D. and V.M. edited the paper; A.D. and V.M. wrote the paper.

This work was supported by National Institutes of Health Grants NS086085 and EB022907. We thank members of the UPENN-RAM consortia for generously sharing their unique iEEG data; Drs. Paul A. Wanda, Michael V. DePalatis, Youssef Ezzyat, Richard Betzel, and Leon A. Davis for assistance with the UPENN-RAM dataset; Drs. Matteo Fraschini and Arjan Hillebrand for generously sharing their MATLAB code for phase transfer entropy analysis; and Dr. Byeongwook Lee for assistance with Figure 1.

The authors declare no competing financial interests.

Correspondence should be addressed to Anup Das at a1das@stanford.edu or Vinod Menon at menon@stanford.edu.

https://doi.org/10.1523/JNEUROSCI.0802-21.2021

Introduction

Hippocampal-prefrontal cortex (PFC) circuits play a critical role in episodic memory in rodents, nonhuman primates, and humans (Eichenbaum, 2017; Rutishauser et al., 2021). Impairments in hippocampal-PFC circuit interactions are prominent in psychiatric and neurologic disorders (Meyer-Lindenberg et al., 2005; Dickerson and Eichenbaum, 2010; Uhlhaas and Singer, 2012), highlighting a critical need for understanding of their electrophysiological mechanisms in the human brain. In the past decade, investigations using noninvasive functional magnetic resonance imaging (fMRI) techniques have provided consistent evidence for

coactivation of the hippocampus and multiple PFC subdivisions during a wide range of tasks involving memory encoding and recall (Rugg and Vilberg, 2013; Moscovitch et al., 2016). However, the electrophysiological basis of dynamic causal hippocampal-PFC interactions in the human brain are poorly understood as fMRI does not have the requisite temporal resolution to address this question. Here, we use data from a large cohort of intracranial EEG (iEEG) recordings to investigate feedforward and feedback causal information flow between the hippocampus and distinct subdivisions of the PFC, and its frequency specificity, during memory encoding and subsequent recall of verbal materials. We operationalize causality as follows: a brain region has a causal influence on a target if knowing the past history of temporal signals in both regions improves the ability to predict the target's signal in comparison to knowing only the target's past (Granger, 1969; Lobier et al., 2014) (see Materials and Methods).

Multiple lines of evidence from studies in rodents and nonhuman primates have pointed to tight anatomic and functional links between hippocampus and PFC as key neural pathways for memory and learning. Anterograde and retrograde tracing studies in rodents have uncovered projections from the hippocampus to the PFC (Jay and Witter, 1991; Hoover and Vertes, 2007). Similarly, studies in rhesus monkeys have demonstrated direct tracts linking the hippocampus to the PFC (Goldman-Rakic et al., 1984; Lavenex and Amaral, 2000). Recent studies using diffusion-weighted imaging and resting-state fMRI have confirmed intrinsic hippocampus connectivity with the PFC in both macaques and humans (Croxson et al., 2005; Qin et al., 2016).

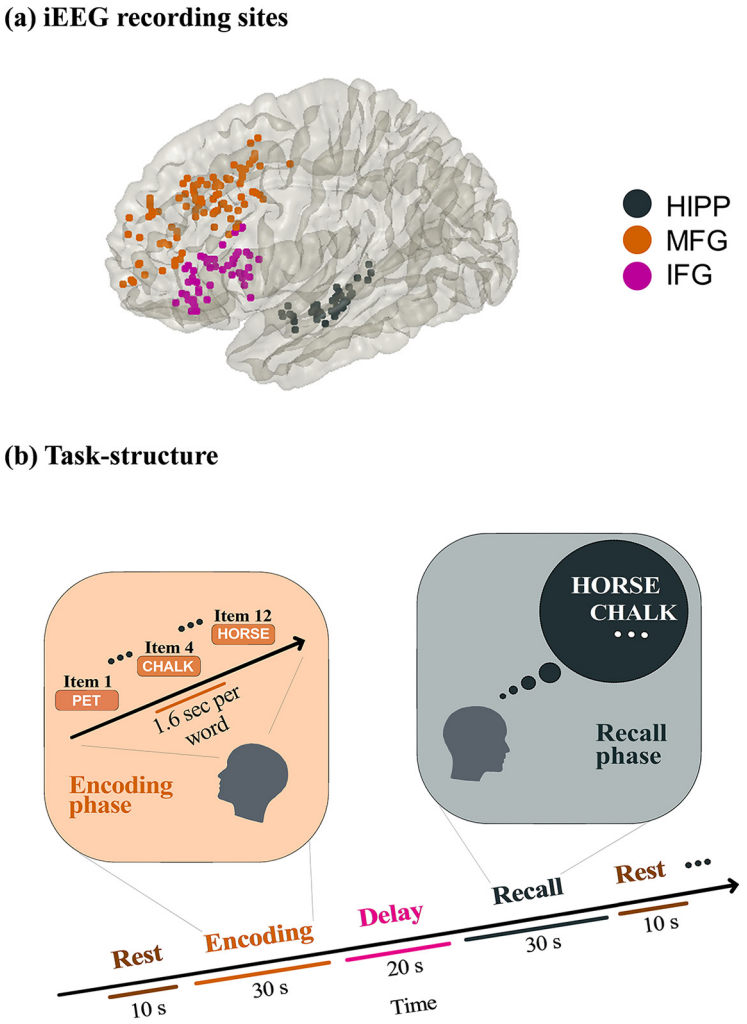

Figure 1. ***a***, iEEG recording sites in hippocampus and two prefrontal cortex subdivisions investigated in this study. ***b***, Event structure and timing of memory encoding and recall task phases. Participants were first presented with a list of words in the encoding block and asked to recall as many as possible from the original list after a short delay (for details, see Materials and Methods). HIPP: hippocampus, MFG: middle frontal gyrus and IFG: inferior frontal gyrus subdivisions of prefrontal cortex.

In conjunction with delineation of anatomic tracts between the hippocampus and PFC, electrophysiological studies in rodents have reported strong theta (4-8 Hz) and delta (0.5-4 Hz) frequency band oscillations in the hippocampus (Siapas et al., 2005; Eichenbaum, 2017; Roy et al., 2017; Schultheiss et al., 2020). Rodent electrophysiological studies have also revealed synchronized activity between hippocampus and PFC in these frequency bands during spatial memory tasks (Simons and Spiers, 2003; Jones and Wilson, 2005; Benchenane et al., 2010; Place et al., 2016; Spiers, 2021). Compared with studies in rodents, the electrophysiological signatures of hippocampal-PFC circuits have been less well investigated in nonhuman primates, but recent reports have emphasized bidirectional information flow between the hippocampus and PFC associated with accurate spatial memory performance (Brincat and Miller, 2015; Cruzado et al., 2020). Together, these findings suggest that coordinated interactions between the hippocampus and PFC are critical for spatial learning and memory across species (Eichenbaum, 2017).

In humans, a large body of fMRI studies have consistently reported coactivation of the hippocampus and multiple PFC regions during both spatial and verbal memory tasks (Dobbins et al., 2002; Simons and Spiers, 2003; Dickerson and Eichenbaum, 2010; Rugg and Vilberg, 2013; Qin et al., 2014; Moscovitch et al., 2016), and hippocampus-PFC coactivation is also associated with better memory performance (Kumaran et al., 2009). Various measures of functional connectivity between the hippocampus and PFC have also been associated with memory recall (van Kesteren et al., 2010; Preston and Eichenbaum, 2013; Qin et al., 2014), but their electrophysiological basis is poorly understood. Studies using noninvasive magnetoencephalography in humans have suggested that hippocampal-PFC coherence in the delta-theta frequency band is associated with successful memory integration (Guitart-Masip et al., 2013; Backus et al., 2016; Spaak and de Lange, 2020). Studies using iEEG have reported increased hippocampal-PFC theta band synchronization associated with spatial memory retrieval (Watrous et al., 2013; Ekstrom and Watrous, 2014; Neuner et al., 2014) and have hinted that a similar process may apply to verbal memory recall as well (Anderson et al., 2010).

Although these studies have provided significant insights into hippocampal and PFC engagement in human episodic memory, the precise pattern of "bottom-up" and "top-down" dynamic causal interactions and frequency-dependent direction of information flow is not known because of the poor temporal

resolution of fMRI and paucity of deep brain electrophysiological data from multiple brain regions. Furthermore, compared with spatial memory, there have been comparatively far fewer investigations of hippocampal-PFC interactions associated with episodic memory encoding and recall of verbal materials, a domain with no equivalents in rodent and nonhuman primate models. To address this challenge, we used iEEG data from the UPENN-RAM study (Solomon et al., 2019), which includes depth recordings sampled at a high temporal resolution of 1 KHz from a large cohort of individuals, to probe the directionality of information flow between the hippocampus and multiple subdivisions of the left lateral PFC.

The first goal of our study was to determine directed causal information flow between the hippocampus and PFC during verbal episodic memory. We investigated the directionality of information flow between these regions during encoding and subsequent recall of a list of words using phase transfer entropy (PTE) (Lobier et al., 2014; Hillebrand et al., 2016; Wang et al., 2017). PTE provides a robust and powerful measure for characterizing information flow between brain regions based on phase coupling; and crucially, it captures linear as well as nonlinear intermittent and nonstationary causal dynamics in iEEG data (Menon et al., 1996; Lobier et al., 2014; Hillebrand et al., 2016).

Our analysis focused on hippocampus interactions with two distinct PFC areas encompassing inferior frontal gyrus (IFG) and middle frontal gyrus (MFG) in left hemisphere regions, which have been implicated in prior fMRI studies of verbal episodic memory (Wagner et al., 2001; Dobbins et al., 2002). We hypothesized that the hippocampus would show directional causal influence on the PFC, compared with resting baseline. We further predicted that causal influences of the hippocampus on the PFC would be stronger, compared with the reverse direction, during memory encoding; in contrast, causal influences of IFG subdivision of the PFC on the hippocampus would be stronger, compared with the reverse direction, during memory recall based on the hypothesized role of this region in controlled memory retrieval (Hasegawa et al., 1999; Wagner et al., 2001; Dobbins et al., 2002; Badre et al., 2005; Badre and Wagner, 2007).

Our second goal was to investigate the frequency specificity of causal interactions between the hippocampus and PFC. Although no consensus has emerged on the role of specific frequencies in synchronization of neural responses between the hippocampus and PFC (Brincat and Miller, 2015; Lam et al., 2016; Moreno et al., 2016; Schoffelen et al., 2017), studies in rodents, nonhuman primates, and humans have pointed to prominent functional roles of the delta-theta rhythm (0.5-8 Hz) in the hippocampus (Watrous et al., 2013; Ekstrom and Watrous, 2014; Neuner et al., 2014) and beta band rhythm (12-30 Hz) in prefrontal and parietal cortices (Brovelli et al., 2004; Engel and Fries, 2010; Spitzer and Haegens, 2017; Stanley et al., 2018; Boran et al., 2019). This has led to the suggestion that delta-theta oscillations may preferentially contribute to synchronization of the hippocampus with the PFC (Ekstrom and Watrous, 2014), while beta band oscillations synchronize the PFC with other cortical and subcortical brain areas (Engel and Fries, 2010; Spitzer and Haegens, 2017). However, the frequency specificity of causal interactions between the hippocampus and PFC in these two frequency bands associated with verbal memory formation has not been directly examined before. Based on the emerging literature, we test the hypothesis that the hippocampus has a stronger feedforward causal influence on the PFC in the delta-theta band, whereas the PFC has stronger "top-down" causal influence on the hippocampus in the beta band.

Table 1. Participant demographic information

Participant ID	Gender	Age
185	M	20
193	M	37
195	M	44
196	M	18
200	M	25
203	F	36
204	F	25
207	F	39
222	F	20
223	F	42
228	F	58
230	F	56
232	M	27
236	F	51
240	F	37
247	F	61
260	F	57
264	F	52
275	M	41
283	F	29
286	F	57
292	F	39
297	M	24
298	F	24
299	M	43
310	M	20

Our analysis revealed novel, behaviorally and functionally relevant, insights into the neurophysiological basis of the human hippocampal-PFC interactions and its role in both memory encoding and recall.

Materials and Methods

UPENN-RAM iEEG recordings. iEEG recordings from 102 patients shared by Kahana and colleagues at the University of Pennsylvania (UPENN) (obtained from the UPENN-RAM public data release under release ID Release_20171012, released on October 12, 2017) were used for analysis (Jacobs et al., 2016). Patients with pharmaco-resistant epilepsy underwent surgery for removal of their seizure onset zones. iEEG recordings of these patients were downloaded from a UPENN-RAM consortium hosted data sharing archive (http://memory.psych.upenn.edu/RAM). Before data collection, research protocols and ethical guidelines were approved by the Institutional Review Board at the participating hospitals, and informed consent was obtained from the participants and guardians (Jacobs et al., 2016). Details of all the recording sessions and data preprocessing procedures are described by Kahana and colleagues (Jacobs et al., 2016). Briefly, iEEG recordings were obtained using subdural grids and strips (contacts placed 10 mm apart) or depth electrodes (contacts spaced 5-10 mm apart) using recording systems at each clinical site. iEEG systems included DeltaMed XlTek (Natus), Grass Telefactor, and Nihon-Kohden EEG systems. Electrodes located in brain lesions or those that corresponded to seizure onset zones or had significant interictal spiking or had broken leads were excluded from analysis.

Anatomical localization of electrode placement was accomplished by coregistering the postoperative CTs with the postoperative MRIs using FSL (FMRIB [Functional MRI of the Brain] Software Library), BET (Brain Extraction Tool), and FLIRT (FMRIB Linear Image Registration Tool) software packages. Preoperative MRIs were used when postoperative MRIs were not available. The resulting contact locations were mapped to MNI space using an indirect stereotactic technique and OsiriX Imaging Software DICOM viewer package. We used the Brainnetome atlas (Fan et al., 2016) to demarcate the IFG, MFG, and the hippocampus (Greicius et al., 2003). Other important brain regions, such as the dorsal anterior cingulate cortex (dACC) and the dorsal

Table 2. Number of electrode pairs used in PTE analysis[a]

Network pairs	No. of electrodes	No. of participants	Participant IDs (gender/age)
HIPP-IFG	98	8	207 (F/39), 223 (F/42), 230 (F/56), 236 (F/51), 240 (F/37), 297 (M/24), 298 (F/24), 299 (M/43)
HIPP-MFG	178	9	195 (M/44), 207 (F/39), 223 (F/42), 228 (F/58), 230 (F/56), 240 (F/37), 247 (F/61), 298 (F/24), 299 (M/43)

[a]HIPP: hippocampus; IFG: inferior frontal gyrus; MFG: middle frontal gyrus.

medial prefrontal cortex (dmPFC), were excluded from analysis because of lack of sufficient electrode placement in these areas. Of 102 individuals, data from 26 individuals (aged from 18-61 years, mean age 37.7 ± 13.7 years, 16 females) were used for subsequent analysis based on electrode placement in IFG, MFG, and the hippocampus. Gender differences were not analyzed in this study because of lack of sufficient male participants for electrode pairs for brain regions (e.g., hippocampus-IFG and hippocampus-MFG had only 2 male patients each; see Table 2).

iEEG signals were sampled at 1000 Hz. The two major concerns when analyzing interactions between closely spaced intracranial electrodes are volume conduction and confounding interactions with the reference electrode (Burke et al., 2013). Hence, bipolar referencing was used to eliminate confounding artifacts and improve the signal-to-noise ratio of the neural signals, consistent with previous studies using UPENN-RAM iEEG data (Burke et al., 2013; Ezzyat et al., 2018). Signals recorded at individual electrodes were converted to a bipolar montage by computing the difference in signal between adjacent electrode pairs on each strip, grid, and depth electrode and the resulting bipolar signals were treated as new "virtual" electrodes originating from the midpoint between each contact pair, identical to procedures in previous studies using UPENN-RAM data (Solomon et al., 2019). Line noise (60 Hz) and its harmonics were removed from the bipolar signals; and finally, each bipolar signal was *Z*-normalized by removing mean and scaling by the standard deviation. For filtering, we used a fourth-order two-way zero phase lag Butterworth filter throughout the analysis.

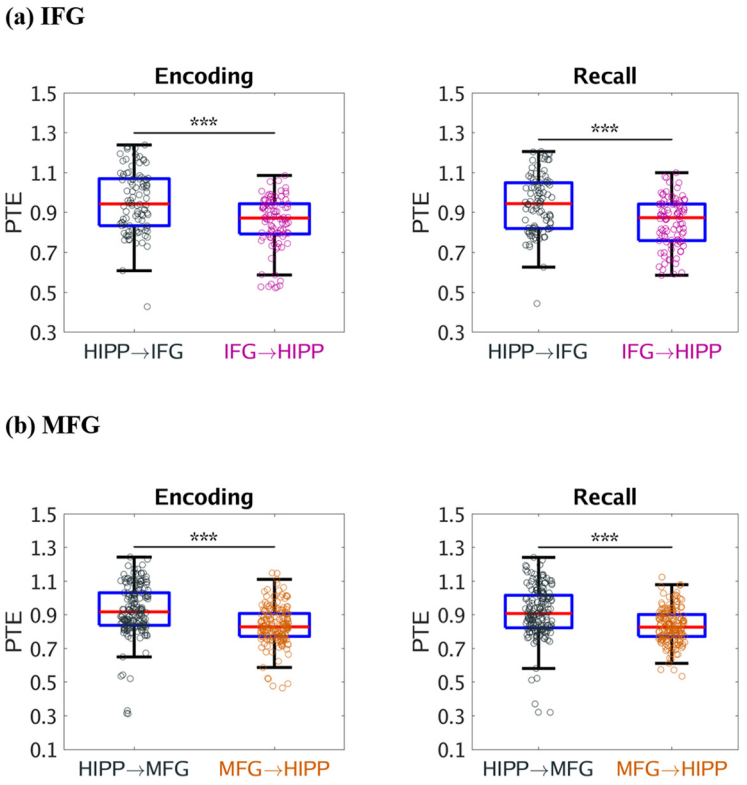

Figure 2. Causal directed information flow between hippocampus and PFC measured using PTE. ***a***, The hippocampus showed higher causal directed information flow to the IFG (HIPP → IFG) during memory encoding and recall, compared with the reverse direction (IFG → HIPP) ($n = 98$). ***b***, The hippocampus also showed higher causal directed information flow to the MFG (HIPP → MFG) during memory encoding and recall, than the reverse direction (MFG → HIPP) ($n = 178$). Only successfully recalled words are included. On each box, the middle mark indicates the median, and the bottom and top edges of the box indicate the 25th and 75th percentiles, respectively. Whiskers extend to the most extreme data points not considered outliers. ***$p < 0.001$ (two-way ANOVA).

iEEG verbal memory encoding and recall, and resting-state task conditions. Patients performed multiple trials of a "free recall" experiment, where they were presented with a list of words and subsequently asked to recall as many as possible from the original list (see Fig. 1). Details of the task are described elsewhere (Solomon et al., 2017, 2019). Average recall accuracy across patients was 25.5 ± 8.7%, similar to prior studies of verbal episodic memory retrieval in neurosurgical patients (Burke et al., 2014). The mismatch in the number trials therefore made it difficult to directly compare causal signaling measures between successfully versus unsuccessfully recalled words. From the point of view of probing behaviorally effective memory encoding, our focus was therefore on successful recall consistent with most prior studies (Watrous et al., 2013; Long et al., 2014). We analyzed iEEG epochs from the encoding and recall periods of the "free recall" task as well as intertrial intervals when participants were given no explicit cognitive task, similar to previous iEEG studies (Miller et al., 2009; Yanagisawa et al., 2012; Horak et al., 2017; Norman et al., 2017). For resting state, we extracted 10 s iEEG recordings (epochs) before the beginning of each trial. To reduce boundary and carryover effects, we discarded 3 s each of iEEG data from the beginning and end of each epoch, resulting in multiple 4 s epochs (Das and Menon, 2020). The encoding and recall epochs were 30 s for each trial. Each encoding trial consisted of 12 words each of 1.6 s duration (see Fig. 1). For the recall periods, iEEG recordings 1.6 s before the vocal onset of each word were analyzed (Solomon et al., 2019). Data from each trial were analyzed separately, and specific measures were averaged across trials. The duration of memory encoding and recall, and resting-state trials were matched to preclude trial-length effects.

iEEG analysis of power spectral density. To calculate average power, we first filtered the iEEG time-series in the frequency band of interest and power, after removing the linear trend, was calculated as the sum of the squares of the amplitudes of the iEEG time-series divided by the length of the time-series.

iEEG analysis of PTE and causal dynamics. PTE is a nonlinear measure of the directionality of information flow between time-series and can be applied as a measure of causality to nonstationary time-series (Lobier et al., 2014). Information flow described here relates to signaling between brain areas and does not necessarily reflect the representation or coding of behaviorally relevant variables per se. The PTE measure is in contrast to the Granger causality measure, which can be applied only to stationary time-series (Barnett and Seth, 2014). We first conducted a stationarity test of the iEEG recordings (unit root test for stationarity) (Barnett and Seth, 2014) and found that the spectral radius of the autoregressive model is very close to 1, indicating that the iEEG time-series is nonstationary. This precluded the applicability of the Granger causality analysis in our study.

Given two time-series $\{x_i\}$ and $\{y_i\}$, where $i = 1, 2, \ldots, M$, instantaneous phases were first extracted using the Hilbert transform. Let $\{x_i^p\}$

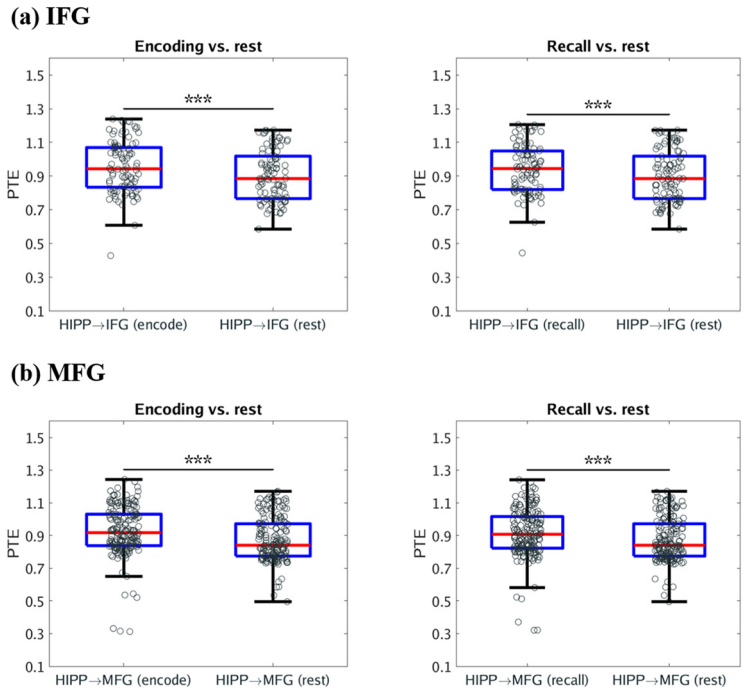

Figure 3. Causal directed information flow from HIPP to PFC during memory encoding and recall, compared with resting state. ***a***, The hippocampus showed higher causal directed information flow to the IFG (HIPP → IFG) during both memory encoding and memory recall, compared with resting-state baseline ($n = 98$). ***b***, The hippocampus also showed higher causal directed information flow to the MFG (HIPP → MFG) during both memory encoding and memory recall, compared with resting-state baseline ($n = 178$). Only successfully recalled words are included. On each box, the middle mark indicates the median, and the bottom and top edges of the box indicate the 25th and 75th percentiles, respectively. Whiskers extend to the most extreme data points not considered outliers. ***$p < 0.001$ (two-way ANOVA).

and $\{y_i^p\}$, where $i = 1, 2, \ldots, M$, denote the corresponding phase time-series. If the uncertainty of the target signal $\{y_i^p\}$at delay τ is quantified using Shannon entropy, then the PTE from driver signal $\{x_i^p\}$ to target signal $\{y_i^p\}$ can be given by the following:

$$PTE_{x\to y} = \sum_i p\left(y_{i+\tau}^p, y_i^p, x_i^p\right)\log\left(\frac{p\left(y_{i+\tau}^p \mid y_i^p, x_i^p\right)}{p\left(y_{i+\tau}^p \mid y_i^p\right)}\right) \quad (1)$$

where the probabilities can be calculated by building histograms of occurrences of singles, pairs, or triplets of instantaneous phase estimates from the phase time-series (Hillebrand et al., 2016). For our analysis, the number of bins in the histograms was set as $3.49 \times \mathrm{SD} \times \mathrm{M}^{-1/3}$ and delay τ was set as 2M/M±, where SD is the average SD of the phase time-series $\{x_i^p\}$ and $\{y_i^p\}$ and M± is the number of times the phase changes sign across time and channels (Hillebrand et al., 2016). PTE has been shown to be robust against the choice of the delay τ and the number of bins for forming the histograms (Hillebrand et al., 2016).

Statistical analysis. Statistical analysis was conducted using mixed-effects analysis with the lmerTest package (Kuznetsova et al., 2017) implemented in R software (version 4.0.2, R Foundation for Statistical Computing). Because PTE data were not normally distributed, we used BestNormalize (Peterson and Cavanaugh, 2018), which contains a suite of transformation-estimating functions that can be used to optimally normalize data. The resulting normally distributed data were subjected to mixed-effects analysis with the following model: $PTE \sim Condition + (1|Subject)$, where *Condition* models the fixed effects (condition differences) and (1|*Subject*) models the random repeated measurements within the same participant. ANOVA was used to test the significance of findings with FDR corrections for multiple comparisons ($p < 0.05$). Similar mixed-effects statistical analysis procedures were used for comparison of power spectral density across task conditions.

Finally, we conducted surrogate analysis to test the significance of the estimated PTE values (Hillebrand et al., 2016). The estimated phases from the Hilbert transform for electrodes from a given pair of brain areas were time-shuffled so that the predictability of one time-series from another is destroyed, and PTE analysis was repeated on these shuffled data to build a distribution of surrogate PTE values against which the observed PTE was tested ($p < 0.05$).

Results

Causal information flow from the hippocampus to PFC during successful memory encoding

We first examined dynamic causal influences of the hippocampus on the IFG and MFG nodes of the PFC during the memory encoding period of a verbal episodic memory task in which participants were presented with a sequence of words and asked to remember them for subsequent recall (see Materials and Methods; Tables 1 and 2; Fig. 1*a*,*b*). Briefly, the task consisted of three periods: encoding, delay, and recall. During encoding, a list of 12 words was visually presented for ~30 s. Words were selected at random, without replacement, from a pool of high frequency English nouns (http://memory.psych.upenn.edu/Word_Pools). Each word was presented for a duration of 1600 ms, followed by an interstimulus interval of 800-1200 ms. After a 20 s postencoding delay, participants were instructed to recall as many words as possible during the 30 s recall period.

We used PTE (Lobier et al., 2014) to compute broadband (0.5-160 Hz) causal influence from the hippocampus to the IFG and MFG in the PFC and vice-versa. During successful memory encoding, the hippocampus had higher broadband causal influences on both the IFG ($F_{(1,187)} = 41.79$, $p < 0.001$) and MFG ($F_{(1,346)} = 80.33$, $p < 0.001$) nodes than the reverse (Fig. 2*a* and Fig. 2*b*, respectively). However, causal influence of the hippocampus on the IFG and MFG nodes did not differ from each other during successful memory encoding ($F_{(1,271)} = 0.11$, $p > 0.05$). Causal influence of the IFG on the hippocampus was higher than the causal influence of the MFG on the hippocampus during successful memory encoding ($F_{(1,274)} = 24.14$, $p < 0.001$). These results demonstrate that the hippocampus has asymmetric causal information flow to both the IFG and MFG during successful memory encoding.

Causal information flow from the hippocampus on PFC during successful memory recall

Next, we examined causal influences of the hippocampus on the PFC during the recall phase of the verbal episodic memory task in which participants recalled the words they had seen during the memory encoding phase (Fig. 1*b*; see Materials and Methods). During successful memory recall, the hippocampus had higher broadband causal influences on both the IFG ($F_{(1,187)} = 40.47$, $p < 0.001$) and MFG ($F_{(1,346)} = 70.69$, $p < 0.001$) than the reverse (Fig. 2*a* and Fig. 2*b*, respectively). However, causal influence of the hippocampus on the IFG and MFG did not differ from each other during

successful memory recall ($F_{(1,271)} = 0.01$, $p > 0.05$). Causal influence of the IFG on the hippocampus was higher than the causal influence of the MFG on the hippocampus during successful memory recall ($F_{(1,274)} = 28.91$, $p < 0.001$). These results demonstrate that the hippocampus has asymmetric causal information flow to both the IFG and MFG subdivisions of the PFC during successful memory recall.

Causal information flow from the hippocampus on PFC during memory encoding and memory recall, compared with resting state

We next investigated changes in causal influences of the hippocampus on the IFG and MFG during memory encoding and recall, compared with the resting state. Our analysis revealed that the causal influences of the hippocampus on the IFG and MFG were higher during both the successful memory encoding and recall task conditions compared with the resting state ($F_{(1,187)} = 28.70$, $F_{(1,187)} = 11.94$, $F_{(1,346)} = 57.65$, $F_{(1,346)} = 32.05$, respectively; $p < 0.001$ in all cases) (Fig. 3). These results demonstrate that the hippocampus has asymmetric causal information flow to both the IFG and MFG during task conditions compared with resting baseline.

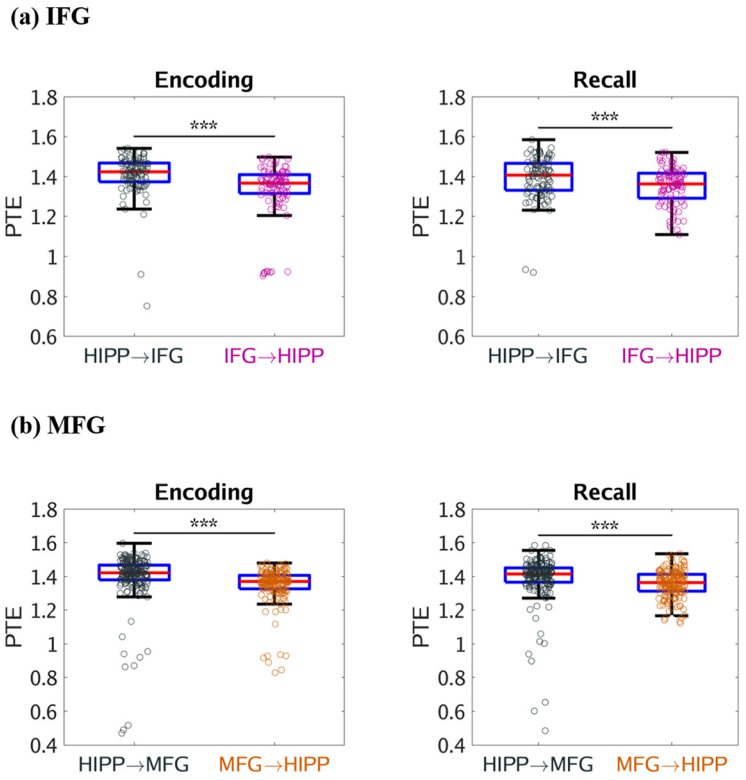

Figure 4. Causal directed information flow between hippocampus and PFC in the delta-theta-alpha (0.5-12 Hz) frequency band. ***a***, Hippocampus → IFG during memory encoding and recall ($n = 98$). ***b***, Hippocampus → MFG during memory encoding and recall ($n = 178$). Hippocampus nodes had higher causal influences on both IFG and MFG nodes than the reverse during both memory encoding and recall in the delta-theta-alpha frequency band. Only successfully recalled words are included. On each box, the middle mark indicates the median, and the bottom and top edges of the box indicate the 25th and 75th percentiles, respectively. Whiskers extend to the most extreme data points not considered outliers. ***$p < 0.001$ (two-way ANOVA).

Causal information flow from the hippocampus to PFC in the delta-theta frequency band

Based on previous findings from iEEG studies which have reported significant delta-theta frequency (0.5-8 Hz) band activity in the hippocampus during recall of verbal, temporal, and spatial information from recently encoded memories and hippocampal-PFC interactions during spatial memory recall (Watrous et al., 2013; Ekstrom and Watrous, 2014; Neuner et al., 2014), we next investigated the dynamic causal influences of the hippocampus on the PFC nodes and vice-versa in the low frequency delta-theta (0.5-8 Hz) band (for results in the 0.5-12 Hz frequency band, see Fig. 4). We computed PTE from the PFC nodes to the hippocampus and, in the reverse direction, during successful memory encoding, and recall in the delta-theta (0.5-8 Hz) frequency band. This analysis revealed that the hippocampus had higher causal influences on the IFG and MFG subdivisions of the PFC than the reverse during both successful memory encoding and recall conditions ($F_{(1,185)} = 30.83$, $F_{(1,186)} = 11.68$, $F_{(1,345)} = 66.30$, $F_{(1,345)} = 48.34$, respectively; $p < 0.001$ in all cases) (Fig. 5). These results demonstrate a key role for delta-theta frequency signaling underlying higher causal influences of the hippocampus on the PFC.

Causal information from the PFC to the hippocampus in the beta frequency band

Next, we examined frequency-specific information flow between the hippocampus and PFC based on emerging findings in nonhuman primates regarding cortical signaling in the beta frequency (12-30 Hz) band during cognition (Engel and Fries, 2010). We computed PTE from the PFC nodes to the hippocampus, and in the reverse direction, during successful memory encoding, and recall in the beta frequency (12-30 Hz) band. This analysis revealed that the IFG had higher causal influences on the hippocampus during both successful memory encoding ($F_{(1,189)} = 62.13$, $p < 0.001$) and recall conditions ($F_{(1,189)} = 24.72$, $p < 0.001$). Similarly, the MFG also had higher causal influences on the hippocampus during both successful memory encoding ($F_{(1,346)} = 59.14$, $p < 0.001$) and recall ($F_{(1,345)} = 6.03$, $p < 0.05$) (Fig. 6). These results demonstrate a key role for beta frequency signaling underlying higher causal influences of both the IFG and MFG subdivisions of the PFC on the hippocampus.

Surrogate data analysis of causal information flow between the hippocampus and the PFC

Finally, we conducted surrogate data analysis to test the significance of the estimated PTE values compared with PTE expected by chance (see Materials and Methods). The estimated phases from the Hilbert transform for electrodes from pairs of brain areas were time-shuffled, and PTE analysis was repeated on these shuffled data to build a distribution of surrogate PTE values against which the observed PTE was tested. This analysis revealed that causal information flow from the hippocampus to the IFG and MFG nodes and the reverse were significantly higher than those expected by chance (Fig. 7) ($p < 0.05$ in all cases) in broadband for both successful memory encoding and recall, indicating bidirectional causal information flow between the hippocampus and the PFC in broadband.

Frequency-specific surrogate data analysis further revealed that causal information flow from the hippocampus to the IFG

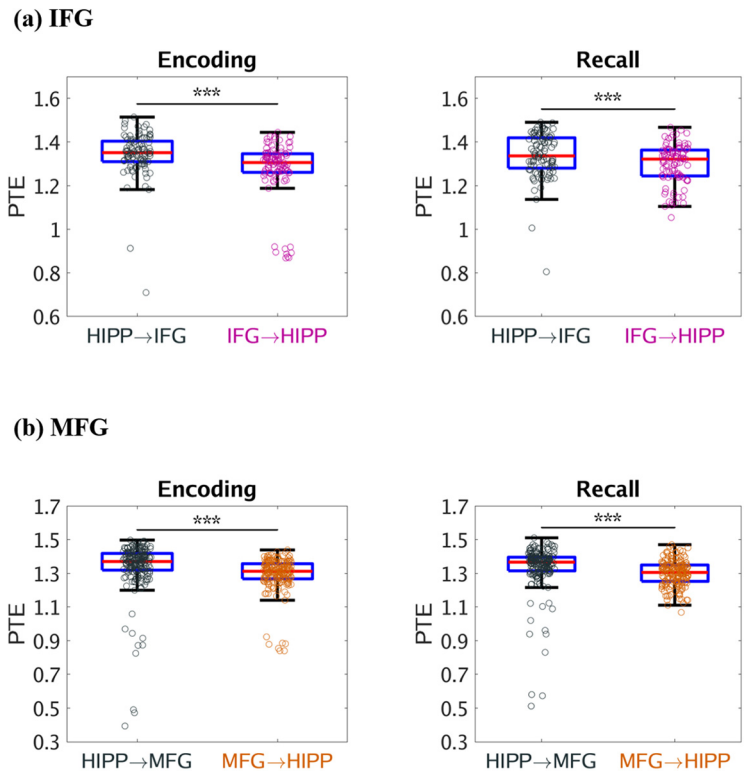

Figure 5. Causal directed information flow from hippocampus to PFC in the delta-theta (0.5-8 Hz) frequency band. ***a***, Causal directed information flow from hippocampus to IFG (HIPP → IFG) was greater during both memory encoding and recall, compared with the reverse direction (IFG → HIPP) ($n = 98$). ***b***, Similarly, causal directed information flow from hippocampus to MFG (HIPP → MFG) was greater during both memory encoding and recall, compared with the reverse direction (MFG → HIPP) ($n = 178$). Only successfully recalled words are included. On each box, the middle mark indicates the median, and the bottom and top edges of the box indicate the 25th and 75th percentiles, respectively. Whiskers extend to the most extreme data points not considered outliers. ***$p < 0.001$ (two-way ANOVA).

and MFG nodes and the reverse were significantly higher than those expected by chance (Fig. 8) ($p < 0.05$ in all cases) in the delta-theta frequency band for both successful memory encoding and recall, indicating bidirectional causal information flow between the hippocampus and the PFC in delta-theta band. Analysis in the beta frequency band revealed that causal information flow from the hippocampus to the IFG and MFG nodes and the reverse were significantly lower than those expected by chance (Fig. 9) ($p < 0.05$ in all cases) for both successful memory encoding and recall, indicating significantly lower predictability of one brain area from the other than expected by chance, in this frequency band.

These results demonstrate that all reported effects in this study arise from causal signaling that is significantly enhanced above chance levels.

Power spectral density during memory encoding and recall compared with resting-state

Finally, we compared the power spectral density (see Materials and Methods; Table 3) in the hippocampus and the IFG and MFG nodes of the PFC across resting-state, memory encoding, and memory recall conditions. As with analyses reported above, the duration of task and rest trials were matched to ensure that differences in network dynamics could not be explained by the differences in the duration of the trials. This analysis revealed that power across the three conditions do not differ from each other in any region (hippocampus/IFG/MFG) (all p values > 0.05).

Previous studies have suggested that power in the high-gamma band (80-160 Hz) is correlated with fMRI BOLD signals (Leopold et al., 2003; Mantini et al., 2007; Scholvinck et al., 2010; Hutchison et al., 2015; Lakatos et al., 2019), and is thought to reflect local activity (Canolty and Knight, 2010). The spectrogram for each brain region, estimated using the short-time Fourier transform (Zhou et al., 2019), confirmed significant high-gamma band activity during both memory encoding and recall (Figs. 10 and 11, respectively). We compared high-gamma band power spectral density (for details, see Materials and Methods) in the hippocampus and the IFG and MFG across resting-state, memory encoding, and memory recall conditions. This analysis revealed that power across the three conditions did not differ from each other in any of the three regions (all p values > 0.05).

Discussion

We examined the electrophysiological basis of directed information flow between the hippocampus and PFC during memory formation in humans using depth iEEG recordings from the UPENN-RAM cohort (Solomon et al., 2019). Leveraging one of the largest samples to date, from 26 participants, 187 electrodes, and 276 electrode pairs, our analysis first focused on broadband signatures of causal interaction, as investigations using canonically defined frequency bands can miss aperiodic (1/f) components that might have major influence on signaling between brain regions (Donoghue et al., 2020). Direction-specific information theoretic analysis revealed that the hippocampus has higher causal influence on both the left hemisphere IFG and MFG subdivisions of the PFC than the reverse, and this pattern was observed during both the encoding and recall phases of the verbal episodic memory task. Causal information flow from the hippocampus to PFC increased significantly during memory processing, compared with resting baseline, and surrogate data analysis revealed that the strength of information flow was significantly above chance levels.

Our analysis further revealed frequency specificity of hippocampus-PFC interactions and a dissociation between feedforward and top-down information flow in the delta-theta and beta bands. We found that feedforward causal influences from the hippocampus to PFC in the delta-theta frequency band were higher, compared with the reverse direction, during both memory encoding and memory recall. In contrast, top-down causal influences from the PFC to hippocampus were higher, compared with the reverse direction, in the beta frequency band during both memory encoding and memory recall. Our findings provide novel insights into asymmetric directionality of information flow between the hippocampus and the PFC during episodic memory formation in the human brain.

Directionality of information flow between the hippocampus and the PFC during verbal memory formation

The first goal of our study was to characterize the directionality of information flow between the hippocampus and the PFC during cognition. Our analysis focused on left hemisphere hippocampus, IFG, and MFG aligned with hemisphere lateralization of verbal episodic and semantic memory processes (Wagner et al., 2001; Dobbins et al., 2002). The left hippocampus and PFC are coactivated during encoding and recall of verbal stimuli in memory (van Kesteren et al., 2010; Preston and Eichenbaum, 2013; Qin et al., 2014). However, the directionality of information flow between the hippocampus and PFC during memory encoding and recall is not well understood as fMRI, the mainstay of hippocampus-PFC investigations in humans, lacks requisite temporal resolution for probing causal circuit dynamics.

To address this question, we used PTE, which provides a robust and powerful tool for characterizing information flow between brain regions based on phase coupling (Lobier et al., 2014; Hillebrand et al., 2016; Wang et al., 2017). We used PTE rather than phase locking or coherence, which have been used previously to probe hippocampal-PFC interactions in rodents (Jones and Wilson, 2005; Benchenane et al., 2010), since phase locking or coherence measures do not probe causal influences and cannot address how one region drives another. Instead, our study examined the direction of information flow between the hippocampus and the PFC using robust estimators of the direction of information flow. PTE assesses with the ability of one time-series to predict future values of other time-series, thus estimating the time-delayed causal influences between the two time-series, whereas phase locking or coherence can only estimate "instantaneous" phase synchronization, but not predict the future time-series. Crucially, PTE is a robust, nonlinear measure of directionality of information flow between time-series (Lobier et al., 2014; Hillebrand et al., 2016). A brain region has a stronger causal influence on a target if knowing the past phase of signals in both regions improves the ability to predict the target's phase compared with knowing only the target's past phase. PTE has several advantages

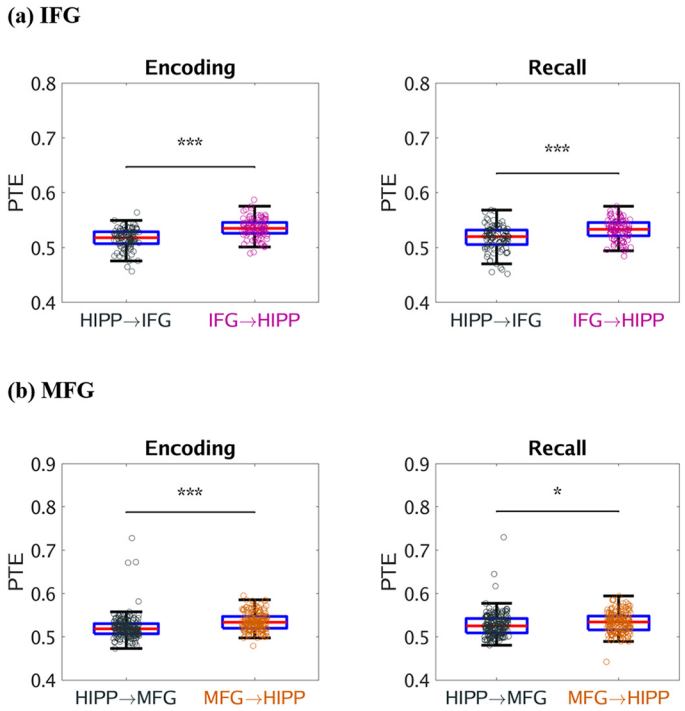

Figure 6. Causal directed information flow between hippocampus and PFC in the beta (12-30 Hz) frequency band. ***a***, Hippocampus → IFG (HIPP → IFG) during memory encoding and recall ($n = 98$). ***b***, Hippocampus → MFG (HIPP → MFG) during memory encoding and recall ($n = 178$). Both IFG and MFG nodes had higher causal influences on the hippocampus than the reverse during both memory encoding and recall in the beta frequency band. Only successfully recalled words are included. On each box, the middle mark indicates the median, and the bottom and top edges of the box indicate the 25th and 75th percentiles, respectively. Whiskers extend to the most extreme data points not considered outliers. ***$p < 0.001$; *$p < 0.05$; (two-way ANOVA).

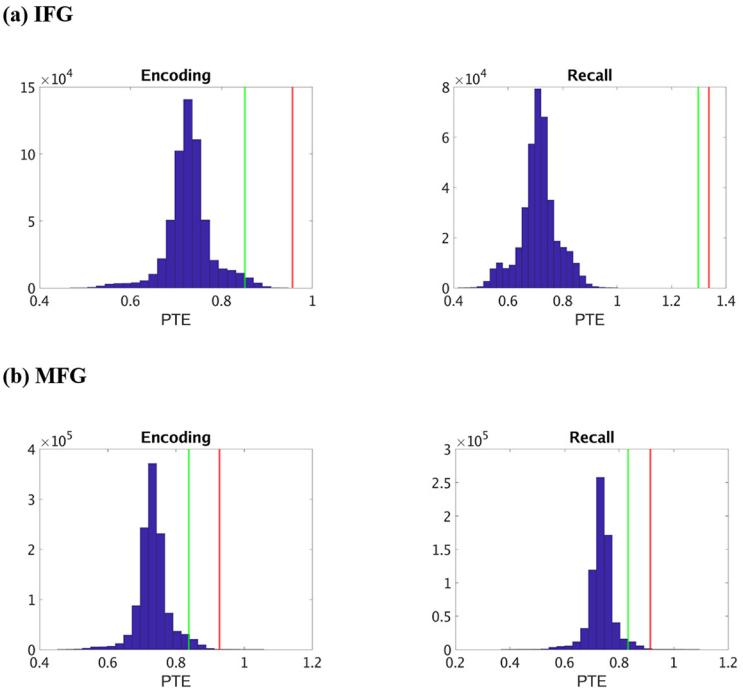

Figure 7. Surrogate data analysis to test the statistical significance of the observed PTE values compared with those obtained by chance in broadband. ***a***, Hippocampus → IFG (HIPP → IFG) during memory encoding and recall. ***b***, Hippocampus → MFG (HIPP → MFG) during memory encoding and recall. Blue represents the distribution of the surrogate PTE values. Red represents the observed PTE for HIPP → IFG/MFG. Green represents the observed PTE for IFG/MFG → HIPP. The estimated phases from the Hilbert transform for a given pair of brain areas were time-shuffled, and PTE analysis was repeated on these shuffled data to build a distribution of surrogate PTE values against which the observed PTE was tested ($p < 0.05$).

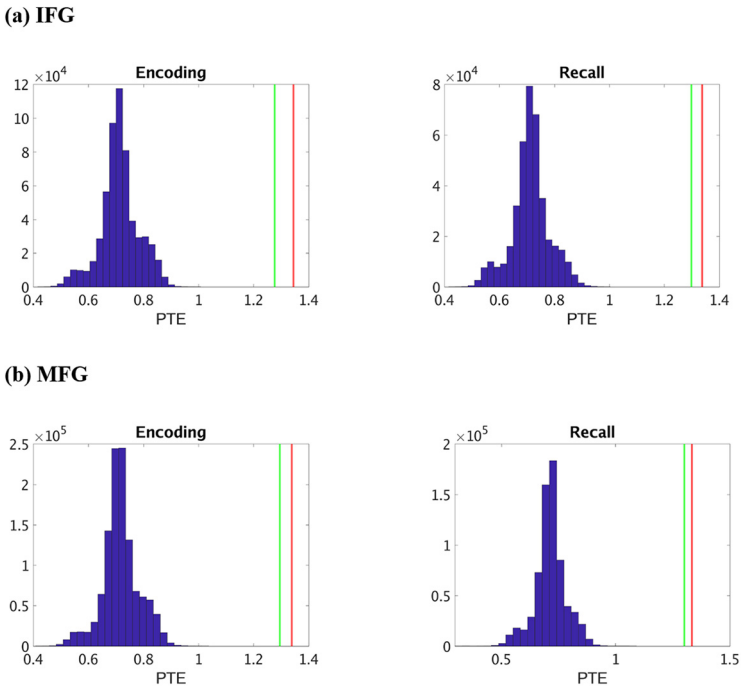

Figure 8. Surrogate data analysis to test the statistical significance of the observed PTE values compared with those obtained by chance in delta-theta band. ***a***, Hippocampus → IFG (HIPP → IFG) during memory encoding and recall. ***b***, Hippocampus → MFG (HIPP → MFG) during memory encoding and recall. Blue represents the distribution of the surrogate PTE values. Red represents the observed PTE for HIPP → IFG/MFG. Green represents the observed PTE for IFG/MFG → HIPP. The estimated phases from the Hilbert transform for a given pair of brain areas were time-shuffled, and PTE analysis was repeated on these shuffled data to build a distribution of surrogate PTE values against which the observed PTE was tested ($p < 0.05$).

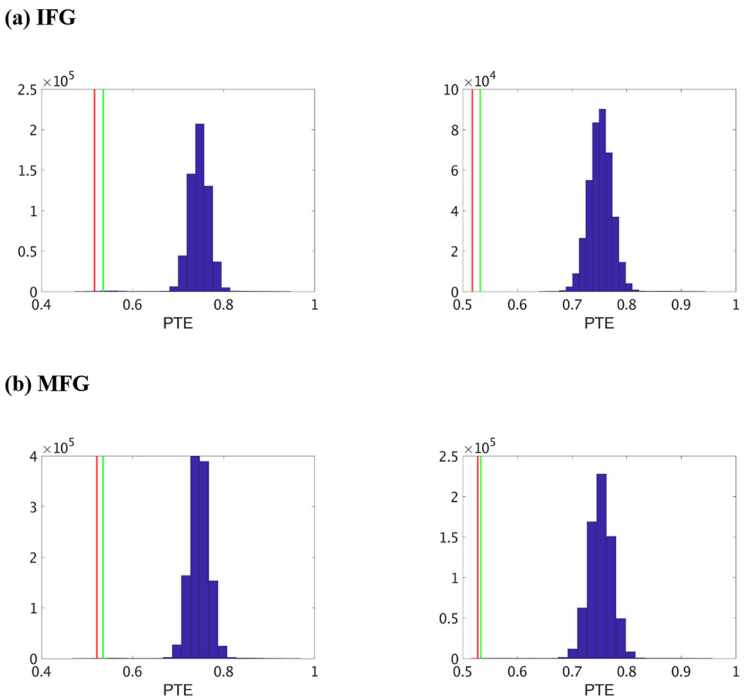

Figure 9. Surrogate data analysis to test the statistical significance of the observed PTE values compared with those obtained by chance in beta band. ***a***, Hippocampus → IFG (HIPP → IFG) during memory encoding and recall. ***b***, Hippocampus → MFG (HIPP → MFG) during memory encoding and recall. Blue represents the distribution of the surrogate PTE values. Red represents the observed PTE for HIPP → IFG/MFG. Green represents the observed PTE for IFG/MFG → HIPP. The estimated phases from the Hilbert transform for a given pair of brain areas were time-shuffled, and PTE analysis was repeated on these shuffled data to build a distribution of surrogate PTE values against which the observed PTE was tested ($p < 0.05$).

over Granger causal analysis (Barnett and Seth, 2014), as it (1) can capture nonlinear interactions, (2) can estimate causality between nonstationary time-series, (3) is more accurate and computationally less expensive than transfer entropy, and (4) estimates causal interactions based on phase, rather than amplitude, coupling (Schreiber, 2000; Lobier et al., 2014; Hillebrand et al., 2016).

We examined causal influences between the hippocampus and the PFC during a verbal episodic memory task in which participants had to subsequently recall a list of words (Solomon et al., 2019). Average recall accuracy across patients was 25.5 ± 8.7%, similar to prior studies of verbal episodic memory retrieval in neurosurgical patients (Burke et al., 2014). The mismatch in the number trials therefore made it difficult to directly compare causal signaling measures between successfully versus unsuccessfully recalled words. From the point of view of probing behaviorally effective memory encoding, our focus was therefore on successful recall consistent with most prior studies (Watrous et al., 2013; Long et al., 2014). Age- or gender-related effects were not analyzed in our study because of lack of sufficient male participants for electrode pairs for brain regions (e.g., hippocampus-IFG and hippocampus-MFG had only 2 male patients each; Table 2).

PTE revealed significantly higher broadband causal influence of the hippocampal electrodes on the IFG and MFG electrodes than the reverse during both successful encoding and successful recall of words in the episodic memory task. Moreover, causal information flow of the hippocampus on the PFC was significantly higher during both memory encoding and recall, compared with the resting state. Our findings are consistent with and extend a previous report in a sample of 3 participants suggesting a trend toward higher causal influence of the hippocampus on bilateral PFC electrodes during episodic memory recall (Anderson et al., 2010). Using a much larger sample of 26 participants localized to the left hemisphere, we found that hippocampal influence on the PFC was significantly higher than the reverse, during both episodic memory encoding and recall. Furthermore, this pattern was observed in both the IFG and MFG subdivisions of the PFC, and causal influences of the hippocampus on the IFG and MFG did not differ from each other,

Table 3. Number of electrodes in each node used in power spectral density analysis[a]

Brain regions	No. of electrodes[b]	No. of participants	Participant IDs (gender/age)
HIPP	44	13	195 (M/44), 203 (F/36), 207 (F/39), 223 (F/42), 228 (F/58), 230 (F/56), 236 (F/51), 240 (F/37), 247 (F/61), 292 (F/39), 297 (M/24), 298 (F/24), 299 (M/43)
IFG	49	13	200 (M/25), 204 (F/25), 207 (F/39), 223 (F/42), 230 (F/56), 236 (F/51), 240 (F/37), 260 (F/57), 264 (F/52), 286 (F/57), 297 (M/24), 298 (F/24), 299 (M/43), 310 (M/20)
MFG	94	21	185 (M/20), 193 (M/37), 195 (M/44), 196 (M/18), 200 (M/25), 204 (F/25), 207 (F/39), 222 (F/20), 223 (F/42), 228 (F/58), 230 (F/56), 232 (M/27), 240 (F/37), 247 (F/61), 260 (F/57), 264 (F/52), 275 (M/41), 283 (F/29), 286 (F/57), 298 (F/24), 299 (M/43)

[a]HIPP: hippocampus; IFG: inferior frontal gyrus; MFG: middle frontal gyrus.
[b]The encoding session file for subject 185 was missing. For the memory encoding task, the number (*n*) of electrodes was 91 for MFG.

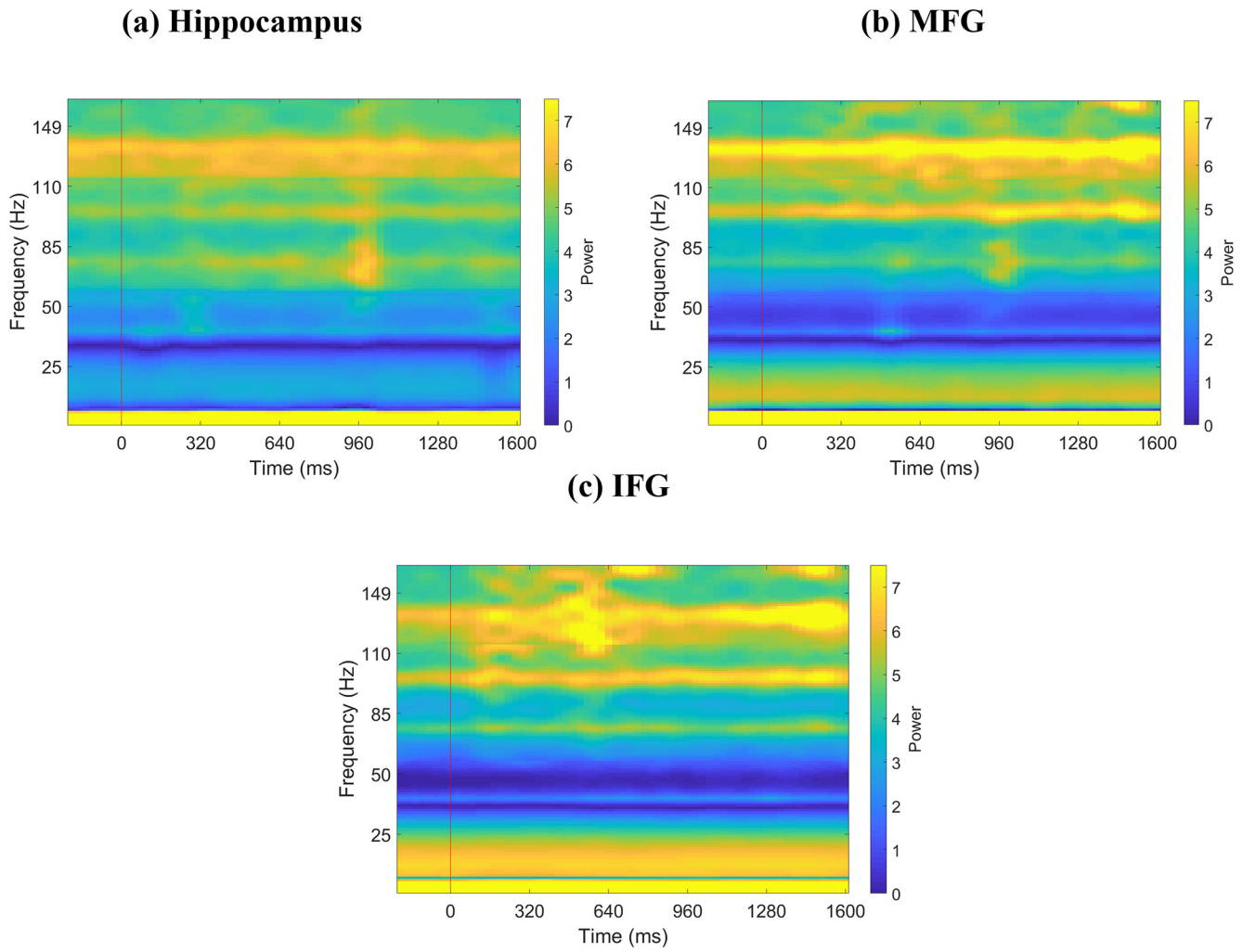

Figure 10. Spectrograms of iEEG activity during memory encoding. ***a***, Hippocampus ($n = 44$). ***b***, MFG ($n = 91$). ***c***, IFG ($n = 49$). Red vertical line indicates presentation of word. Each word was presented for ~1.6 s. Line frequencies have been removed from *y* axis, and *y* axis has been adjusted accordingly for visualization.

neither during successful memory encoding nor during successful memory recall. Although previous fMRI studies have emphasized a greater role for the left IFG in controlled recall of verbal materials (Hasegawa et al., 1999; Wagner et al., 2001; Dobbins et al., 2002; Badre et al., 2005; Badre and Wagner, 2007), the present iEEG findings point to involvement of both the IFG and MFG. Our findings thus provide robust electrophysiological evidence for dynamic causal influence of the hippocampus on both the IFG and MFG subdivisions of the PFC during both memory encoding and recall.

Frequency-specific directionality of information flow between the hippocampus and the PFC

The second goal of our study was to investigate the frequency specificity of directional information flow between the hippocampus and the PFC. Based on previous reports in rodents and nonhuman primates, we focused on delta-theta (0.5-8 Hz) and beta (12-30 Hz) bands, as enhanced local field potentials in these frequency bands have been identified in the hippocampus and PFC, respectively (Engel and Fries, 2010; Watrous et al., 2013; Ekstrom and Watrous, 2014; Stanley et al., 2018; Boran et al., 2019). Previous iEEG studies have reported significant delta-

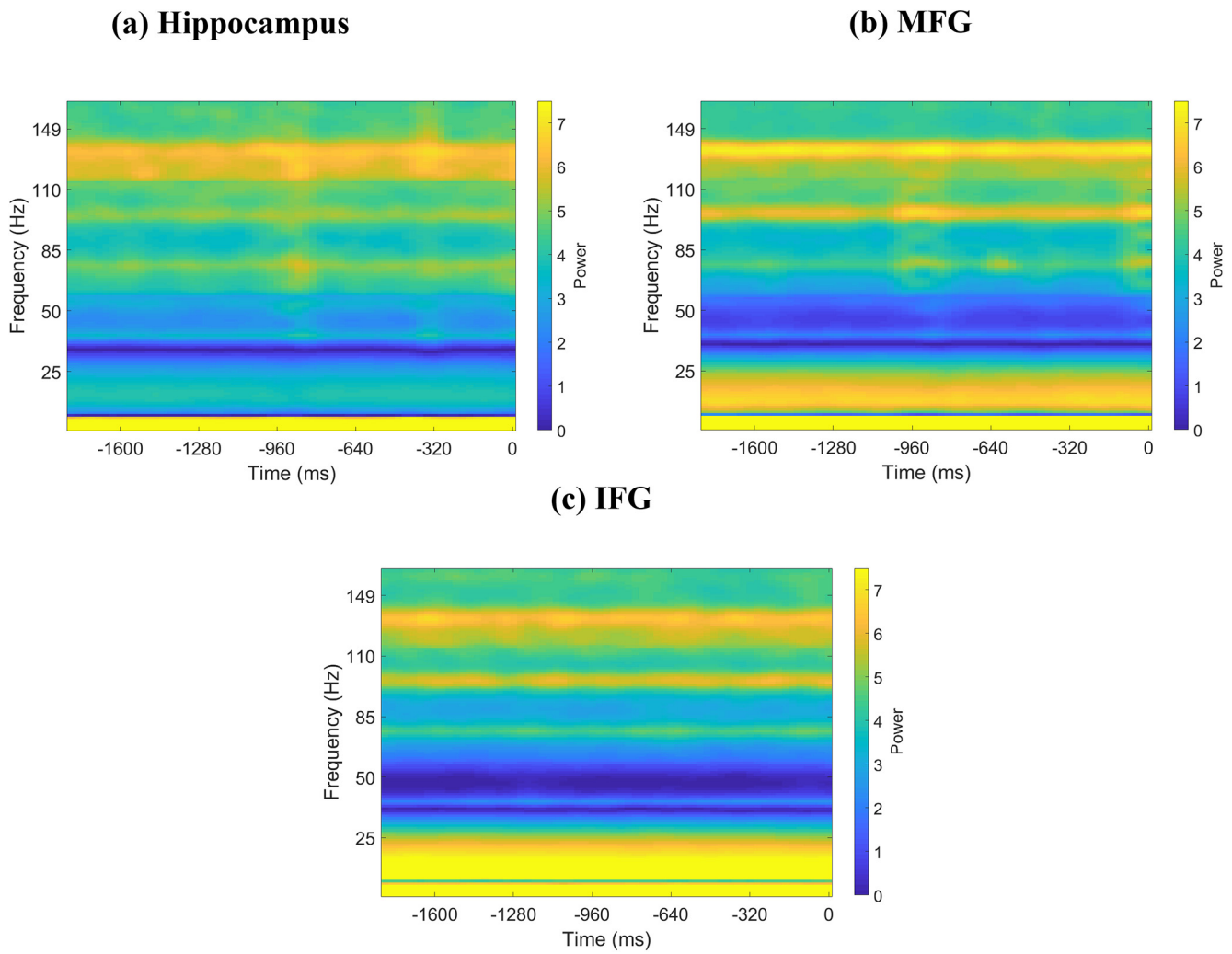

Figure 11. Spectrograms of iEEG activity during memory recall. ***a***, Hippocampus ($n = 44$). ***b***, MFG ($n = 94$). ***c***, IFG ($n = 49$). Zero in the *x* axis denotes recall of a word. Shown is 1.8 s segment immediately preceding recall of a word for each brain region; 1.6 s segment immediately preceding vocal onset of a word was considered for analysis. Line frequencies have been removed from *y* axis, and *y* axis has been adjusted accordingly for visualization.

theta frequency (0.5-8 Hz) band activity in the hippocampus during recall of verbal, temporal, and spatial information from recently encoded memories (Foster et al., 2013; Jacobs et al., 2016; Goyal et al., 2018; Solomon et al., 2019), but the frequency specificity of causal hippocampal-PFC signaling in the human brain associated with memory encoding and recall has not been well understood. Our analysis revealed two key dissociations in the frequency-specific directionality of information flow between the hippocampus and PFC.

In the delta-theta band, we found that the hippocampus had higher causal influences on the PFC, compared with the reverse direction; this pattern was observed during both verbal memory encoding and memory recall. This finding is consistent with reports of delta-theta frequency band hippocampal-PFC synchronization during spatial memory recall (Watrous et al., 2013; Ekstrom and Watrous, 2014; Bohbot et al., 2017). Crucially, we extend previous reports by demonstrating directed causal influences from the hippocampus to PFC during verbal memory processing. In contrast, we found an opposite pattern in the beta band with higher PFC causal influences on the hippocampus, compared with the reverse direction; again, this pattern was observed during both memory encoding and recall.

The pattern of frequency-specific directed causal information flow observed in the present study converges surprisingly well on findings from electrocorticogram recordings in a hierarchy of left hemisphere primate visual areas (Bastos et al., 2015). In this study, which involved 2 macaque monkeys performing a visuospatial attention task, it was found that feedforward influences were carried by delta-theta band synchronization, while feedback influences were carried by beta band synchronization. Furthermore, theta rhythms promoted information flow in the feedforward direction during bottom-up processing, whereas beta rhythms promoted information flow in the reverse direction because beta influences in the top-down direction were significantly diminished when attention was directed away to the left (ipsilateral) visual field. Our findings indicate a similar pattern of frequency-specific directed causal information flow linking hierarchical inflow between the hippocampus and PFC. Top-down information flow from the PFC in the beta band may contribute to transitioning latent neuronal ensembles into "active" representations (Spitzer and Haegens, 2017) as well as the subsequent maintenance of information in cell assemblies (Engel and Fries, 2010), while delta-theta rhythms in the hippocampus may signal pattern completion associated with memory recall that is conveyed to multiple PFC regions (Eichenbaum, 2017).

In sum, these results suggest that the hippocampus and PFC exert feedforward and feedback influences through distinct frequency channels and that delta-theta and beta rhythms have different synchronization properties. This frequency-dependent directionality of information flow may provide a mechanism by which hippocampus and PFC circuits function in concert albeit via parallel signaling mechanism pathways, which reflect their distinct roles in episodic memory formation.

PTE, rather than power spectral density, underlies causal information flow

PTE, as used in the present study, provides a robust measure of direction of information flow between electrode pairs (Lobier et al., 2014; Hillebrand et al., 2016). Previous findings using multielectrode array recordings in both humans and animal models have established that phase, rather than amplitude, is crucial for both spatial and temporal encoding of information in the brain (Lachaux et al., 1999; Kayser et al., 2009; Siegel et al., 2009; Lopour et al., 2013; Ng et al., 2013). Consistent with this, we found no differences in overall power across the three conditions (resting-state, memory encoding, and memory recall) in any of the three brain regions (hippocampus, MFG, and IFG) examined here. Together, these results suggest that PTE, rather than power spectral density, underlies causal information flow reported here.

Signal propagation and temporal delays between the hippocampus and PFC

Across all hippocampus-PFC electrode pairs, the propagation delay τ between the source and target signal estimated by the PTE analysis was 17.7 ms. τ here corresponds to the mean temporal distance between phase reversals across all electrode pairs (see Materials and Methods). This delay refers to the embedding delay used in the PTE analysis, and does not necessarily correspond to the signal propagation delay. Nevertheless, a back of the envelope calculation indicates a close correspondence between the two. The average interelectrode (Euclidean) distance between hippocampus and PFC electrodes in our study was 70.5 mm (actual white matter tracts will be longer). Histologic studies of axonal tracts in primate lateral PFC have suggested a conduction velocity of ~5.4 mm/ms (Caminiti et al., 2013). This results in an axonal transmission time of 13.05 ms, which together with a synaptic transduction time of 3-5 ms matches the delay τ used in the PTE analysis quite well. Thus, the temporal delays used in our study are physiologically meaningful and correspond to directional hippocampus-PFC signal interactions on a timescale consistent with monosynaptic influence.

In conclusion, our study advances foundational knowledge of directed information flow between the hippocampus and PFC during verbal episodic memory in humans. Using high temporal resolution iEEG recordings from a large cohort of participants, we uncovered distinct feedforward and feedback signaling mechanisms between the hippocampus and PFC. Our study also revealed frequency specificity of causal feedforward and feedback interactions between the hippocampus and PFC. Our findings provide novel insights into dynamic causal interactions that subserve episodic memory in the human brain and help advance knowledge of the operating principles of circuit mechanisms in verbal memory encoding and recall. More broadly, our findings provide a template for probing the neural circuit basis of hippocampal-PFC dysfunctions, which are prominent in psychiatric and neurological disorders.

References

Anderson KL, Rajagovindan R, Ghacibeh GA, Meador KJ, Ding M (2010) Theta oscillations mediate interaction between prefrontal cortex and medial temporal lobe in human memory. Cereb Cortex 20:1604–1612.

Backus AR, Schoffelen JM, Szebenyi S, Hanslmayr S, Doeller CF (2016) Hippocampal-prefrontal theta oscillations support memory integration. Curr Biol 26:450–457.

Badre D, Poldrack RA, Paré-Blagoev EJ, Insler RZ, Wagner AD (2005) Dissociable controlled retrieval and generalized selection mechanisms in ventrolateral prefrontal cortex. Neuron 47:907–918.

Badre D, Wagner AD (2007) Left ventrolateral prefrontal cortex and the cognitive control of memory. Neuropsychologia 45:2883–2901.

Barnett L, Seth AK (2014) The MVGC multivariate Granger causality toolbox: a new approach to Granger-causal inference. J Neurosci Methods 223:50–68.

Bastos AM, Vezoli J, Bosman CA, Schoffelen JM, Oostenveld R, Dowdall JR, De Weerd P, Kennedy H, Fries P (2015) Visual areas exert feedforward and feedback influences through distinct frequency channels. Neuron 85:390–401.

Benchenane K, Peyrache A, Khamassi M, Tierney PL, Gioanni Y, Battaglia FP, Wiener SI (2010) Coherent theta oscillations and reorganization of spike timing in the hippocampal-prefrontal network upon learning. Neuron 66:921–936.

Bohbot VD, Copara MS, Gotman J, Ekstrom AD (2017) Low-frequency theta oscillations in the human hippocampus during real-world and virtual navigation. Nat Commun 8:14415.

Boran E, Fedele T, Klaver P, Hilfiker P, Stieglitz L, Grunwald T, Sarnthein J (2019) Persistent hippocampal neural firing and hippocampal-cortical coupling predict verbal working memory load. Sci Adv 5:eaav3687.

Brincat SL, Miller EK (2015) Frequency-specific hippocampal-prefrontal interactions during associative learning. Nat Neurosci 18:576–581.

Brovelli A, Ding M, Ledberg A, Chen Y, Nakamura R, Bressler SL (2004) Beta oscillations in a large-scale sensorimotor cortical network: directional influences revealed by Granger causality. Proc Natl Acad Sci USA 101:9849–9854.

Burke JF, Sharan AD, Sperling MR, Ramayya AG, Evans JJ, Healey MK, Beck EN, Davis KA, Lucas TH, Kahana MJ (2014) Theta and high-frequency activity mark spontaneous recall of episodic memories. J Neurosci 34:11355–11365.

Burke JF, Zaghloul KA, Jacobs J, Williams RB, Sperling MR, Sharan AD, Kahana MJ (2013) Synchronous and asynchronous theta and gamma activity during episodic memory formation. J Neurosci 33:292–304.

Caminiti R, Carducci F, Piervincenzi C, Battaglia-Mayer A, Confalone G, Visco-Comandini F, Pantano P, Innocenti GM (2013) Diameter, length, speed, and conduction delay of callosal axons in macaque monkeys and humans: comparing data from histology and magnetic resonance imaging diffusion tractography. J Neurosci 33:14501–14511.

Canolty RT, Knight RT (2010) The functional role of cross-frequency coupling. Trends Cogn Sci 14:506–515.

Croxson PL, Johansen-Berg H, Behrens TE, Robson MD, Pinsk MA, Gross CG, Richter W, Richter MC, Kastner S, Rushworth MF (2005) Quantitative investigation of connections of the prefrontal cortex in the human and macaque using probabilistic diffusion tractography. J Neurosci 25:8854–8866.

Cruzado NA, Tiganj Z, Brincat SL, Miller EK, Howard MW (2020) Conjunctive representation of what and when in monkey hippocampus and lateral prefrontal cortex during an associative memory task. Hippocampus 30:1332–1346.

Das A, Menon V (2020) Spatiotemporal integrity and spontaneous nonlinear dynamic properties of the salience network revealed by human intracranial electrophysiology: a multicohort replication. Cereb Cortex 30:5309–5321.

Dickerson BC, Eichenbaum H (2010) The episodic memory system: neurocircuitry and disorders. Neuropsychopharmacology 35:86–104.

Dobbins IG, Foley H, Schacter DL, Wagner AD (2002) Executive control during episodic retrieval: multiple prefrontal processes subserve source memory. Neuron 35:989–996.

Donoghue T, Haller M, Peterson EJ, Varma P, Sebastian P, Gao R, Noto T, Lara AH, Wallis JD, Knight RT, Shestyuk A, Voytek B (2020) Parameterizing neural power spectra into periodic and aperiodic components. Nat Neurosci 23:1655–1665.

Eichenbaum H (2017) Prefrontal-hippocampal interactions in episodic memory. Nat Rev Neurosci 18:547–558.
Ekstrom AD, Watrous AJ (2014) Multifaceted roles for low-frequency oscillations in bottom-up and top-down processing during navigation and memory. Neuroimage 85:667–677.
Engel AK, Fries P (2010) Beta-band oscillations: signalling the status quo? Curr Opin Neurobiol 20:156–165.
Ezzyat Y, Wanda PA, Levy DF, Kadel A, Aka A, Pedisich I, Sperling MR, Sharan AD, Lega BC, Burks A, Gross RE, Inman CS, Jobst BC, Gorenstein MA, Davis KA, Worrell GA, Kucewicz MT, Stein JM, Gorniak R, Das SR, et al. (2018) Closed-loop stimulation of temporal cortex rescues functional networks and improves memory. Nat Commun 9:365.
Fan L, Li H, Zhuo J, Zhang Y, Wang J, Chen L, Yang Z, Chu C, Xie S, Laird AR, Fox PT, Eickhoff SB, Yu C, Jiang T (2016) The Human Brainnetome atlas: a new brain atlas based on connectional architecture. Cereb Cortex 26:3508–3526.
Foster BL, Kaveh A, Dastjerdi M, Miller KJ, Parvizi J (2013) Human retrosplenial cortex displays transient theta phase locking with medial temporal cortex prior to activation during autobiographical memory retrieval. J Neurosci 33:10439–10446.
Goldman-Rakic PS, Selemon LD, Schwartz ML (1984) Dual pathways connecting the dorsolateral prefrontal cortex with the hippocampal formation and parahippocampal cortex in the rhesus monkey. Neuroscience 12:719–743.
Goyal A, Miller J, Watrous AJ, Lee SA, Coffey T, Sperling MR, Sharan A, Worrell G, Berry B, Lega B, Jobst BC, Davis KA, Inman C, Sheth SA, Wanda PA, Ezzyat Y, Das SR, Stein J, Gorniak R, Jacobs J (2018) Electrical stimulation in hippocampus and entorhinal cortex impairs spatial and temporal memory. J Neurosci 38:4471–4481.
Granger CW (1969) Investigating causal relations by econometric models and cross-spectral methods. Econometrica 37:424–438.
Greicius MD, Krasnow B, Boyett-Anderson JM, Eliez S, Schatzberg AF, Reiss AL, Menon V (2003) Regional analysis of hippocampal activation during memory encoding and retrieval: fMRI study. Hippocampus 13:164–174.
Guitart-Masip M, Barnes GR, Horner A, Bauer M, Dolan RJ, Duzel E (2013) Synchronization of medial temporal lobe and prefrontal rhythms in human decision making. J Neurosci 33:442–451.
Hasegawa I, Hayashi T, Miyashita Y (1999) Memory retrieval under the control of the prefrontal cortex. Ann Med 31:380–387.
Hillebrand A, Tewarie P, van Dellen E, Yu M, Carbo EW, Douw L, Gouw AA, van Straaten EC, Stam CJ (2016) Direction of information flow in large-scale resting-state networks is frequency-dependent. Proc Natl Acad Sci USA 113:3867–3872.
Hoover WB, Vertes RP (2007) Anatomical analysis of afferent projections to the medial prefrontal cortex in the rat. Brain Struct Funct 212:149–179.
Horak PC, Meisenhelter S, Song Y, Testorf ME, Kahana MJ, Viles WD, Bujarski KA, Connolly AC, Robbins AA, Sperling MR, Sharan AD, Worrell GA, Miller LR, Gross RE, Davis KA, Roberts DW, Lega B, Sheth SA, Zaghloul KA, Stein JM, et al. (2017) Interictal epileptiform discharges impair word recall in multiple brain areas. Epilepsia 58:373–380.
Hutchison RM, Hashemi N, Gati JS, Menon RS, Everling S (2015) Electrophysiological signatures of spontaneous BOLD fluctuations in macaque prefrontal cortex. Neuroimage 113:257–267.
Jacobs J, Miller J, Lee SA, Coffey T, Watrous AJ, Sperling MR, Sharan A, Worrell G, Berry B, Lega B, Jobst BC, Davis K, Gross RE, Sheth SA, Ezzyat Y, Das SR, Stein J, Gorniak R, Kahana MJ, Rizzuto DS (2016) Direct electrical stimulation of the human entorhinal region and hippocampus impairs memory. Neuron 92:983–990.
Jay TM, Witter MP (1991) Distribution of hippocampal CA1 and subicular efferents in the prefrontal cortex of the rat studied by means of anterograde transport of Phaseolus vulgaris-leucoagglutinin. J Comp Neurol 313:574–586.
Jones MW, Wilson MA (2005) Theta rhythms coordinate hippocampal-prefrontal interactions in a spatial memory task. PLoS Biol 3:e402.
Kayser C, Montemurro MA, Logothetis NK, Panzeri S (2009) Spike-phase coding boosts and stabilizes information carried by spatial and temporal spike patterns. Neuron 61:597–608.
Kumaran D, Summerfield JJ, Hassabis D, Maguire EA (2009) Tracking the emergence of conceptual knowledge during human decision making. Neuron 63:889–901.
Kuznetsova A, Brockhoff PB, Christensen RH (2017) lmerTest package: tests in linear mixed-effects models. J Stat Soft 82:1–26.
Lachaux JP, Rodriguez E, Martinerie J, Varela FJ (1999) Measuring phase synchrony in brain signals. Hum Brain Mapp 8:194–208.
Lakatos P, Gross J, Thut G (2019) A new unifying account of the roles of neuronal entrainment. Curr Biol 29:R890–R905.
Lam NH, Schoffelen JM, Udden J, Hulten A, Hagoort P (2016) Neural activity during sentence processing as reflected in theta, alpha, beta, and gamma oscillations. Neuroimage 142:43–54.
Lavenex P, Amaral DG (2000) Hippocampal-neocortical interaction: a hierarchy of associativity. Hippocampus 10:420–430.
Leopold DA, Murayama Y, Logothetis NK (2003) Very slow activity fluctuations in monkey visual cortex: implications for functional brain imaging. Cereb Cortex 13:422–433.
Lobier M, Siebenhühner F, Palva S, Matias PJ (2014) Phase transfer entropy: a novel phase-based measure for directed connectivity in networks coupled by oscillatory interactions. Neuroimage 85:853–872.
Long NM, Burke JF, Kahana MJ (2014) Subsequent memory effect in intracranial and scalp EEG. Neuroimage 84:488–494.
Lopour BA, Tavassoli A, Fried I, Ringach DL (2013) Coding of information in the phase of local field potentials within human medial temporal lobe. Neuron 79:594–606.
Mantini D, Perrucci MG, Del Gratta C, Romani GL, Corbetta M (2007) Electrophysiological signatures of resting state networks in the human brain. Proc Natl Acad Sci USA 104:13170–13175.
Menon V, Freeman WJ, Cutillo BA, Desmond JE, Ward MF, Bressler SL, Laxer KD, Barbaro N, Gevins AS (1996) Spatio-temporal correlations in human gamma band electrocorticograms. Electroencephalogr Clin Neurophysiol 98:89–102.
Meyer-Lindenberg AS, Olsen RK, Kohn PD, Brown T, Egan MF, Weinberger DR, Berman KF (2005) Regionally specific disturbance of dorsolateral prefrontal-hippocampal functional connectivity in schizophrenia. Arch Gen Psychiatry 62:379–386.
Miller KJ, Weaver KE, Ojemann JG (2009) Direct electrophysiological measurement of human default network areas. Proc Natl Acad Sci USA 106:12174–12177.
Moreno A, Morris RG, Canals S (2016) Frequency-dependent gating of hippocampal-neocortical interactions. Cereb Cortex 26:2105–2114.
Moscovitch M, Cabeza R, Winocur G, Nadel L (2016) Episodic memory and beyond: the hippocampus and neocortex in transformation. Annu Rev Psychol 67:105–134.
Neuner I, Arrubla J, Werner CJ, Hitz K, Boers F, Kawohl W, Shah NJ (2014) The default mode network and EEG regional spectral power: a simultaneous fMRI-EEG study. PLoS One 9:e88214.
Ng BS, Logothetis NK, Kayser C (2013) EEG phase patterns reflect the selectivity of neural firing. Cereb Cortex 23:389–398.
Norman Y, Yeagle EM, Harel M, Mehta AD, Malach R (2017) Neuronal baseline shifts underlying boundary setting during free recall. Nat Commun 8:1301.
Peterson RA, Cavanaugh JE (2018) Ordered quantile normalization: a semiparametric transformation built for the cross-validation era. J Appl Statistics 82:2312–2327.
Place R, Farovik A, Brockmann M, Eichenbaum H (2016) Bidirectional prefrontal-hippocampal interactions support context-guided memory. Nat Neurosci 19:992–994.
Preston AR, Eichenbaum H (2013) Interplay of hippocampus and prefrontal cortex in memory. Curr Biol 23:R764–R773.
Qin S, Cho S, Chen T, Rosenberg-Lee M, Geary DC, Menon V (2014) Hippocampal-neocortical functional reorganization underlies children's cognitive development. Nat Neurosci 17:1263–1269.
Qin S, Duan X, Supekar K, Chen H, Chen T, Menon V (2016) Large-scale intrinsic functional network organization along the long axis of the human medial temporal lobe. Brain Struct Funct 221:3237–3258.
Roy A, Svensson FP, Mazeh A, Kocsis B (2017) Prefrontal-hippocampal coupling by theta rhythm and by 2-5 Hz oscillation in the delta band: the role of the nucleus reuniens of the thalamus. Brain Struct Funct 222:2819–2830.
Rugg MD, Vilberg KL (2013) Brain networks underlying episodic memory retrieval. Curr Opin Neurobiol 23:255–260.
Rutishauser U, Reddy L, Mormann F, Sarnthein J (2021) The architecture of human memory: insights from human single-neuron recordings. J Neurosci 41:883–890.

Schoffelen JM, Hulten A, Lam N, Marquand AF, Udden J, Hagoort P (2017) Frequency-specific directed interactions in the human brain network for language. Proc Natl Acad Sci USA 114:8083–8088.

Scholvinck ML, Maier A, Ye FQ, Duyn JH, Leopold DA (2010) Neural basis of global resting-state fMRI activity. Proc Natl Acad Sci USA 107:10238–10243.

Schreiber T (2000) Measuring information transfer. Phys Rev Lett 85:461–464.

Schultheiss NW, Schlecht M, Jayachandran M, Brooks DR, McGlothan JL, Guilarte TR, Allen TA (2020) Awake delta and theta-rhythmic hippocampal network modes during intermittent locomotor behaviors in the rat. Behav Neurosci 134:529–546.

Siapas AG, Lubenov EV, Wilson MA (2005) Prefrontal phase locking to hippocampal theta oscillations. Neuron 46:141–151.

Siegel M, Warden MR, Miller EK (2009) Phase-dependent neuronal coding of objects in short-term memory. Proc Natl Acad Sci USA 106:21341–21346.

Simons JS, Spiers HJ (2003) Prefrontal and medial temporal lobe interactions in long-term memory. Nat Rev Neurosci 4:637–648.

Solomon EA, Kragel JE, Sperling MR, Sharan A, Worrell G, Kucewicz M, Inman CS, Lega B, Davis KA, Stein JM, Jobst BC, Zaghloul KA, Sheth SA, Rizzuto DS, Kahana MJ (2017) Widespread theta synchrony and high-frequency desynchronization underlies enhanced cognition. Nat Commun 8:1704.

Solomon EA, Stein JM, Das S, Gorniak R, Sperling MR, Worrell G, Inman CS, Tan RJ, Jobst BC, Rizzuto DS, Kahana MJ (2019) Dynamic theta networks in the human medial temporal lobe support episodic memory. Curr Biol 29:1100–1111.e1104.

Spaak E, de Lange FP (2020) Hippocampal and prefrontal theta-band mechanisms underpin implicit spatial context learning. J Neurosci 40:191–202.

Spiers HJ (2021) Brain rhythms that help us to detect borders. Nature 589:353–354.

Spitzer B, Haegens S (2017) Beyond the status quo: a role for beta oscillations in endogenous content (re)activation. eNeuro 4: ENEURO.0170-17.2017.

Stanley DA, Roy JE, Aoi MC, Kopell NJ, Miller EK (2018) Low-beta oscillations turn up the gain during category judgments. Cereb Cortex 28:116–130.

Uhlhaas PJ, Singer W (2012) Neuronal dynamics and neuropsychiatric disorders: toward a translational paradigm for dysfunctional large-scale networks. Neuron 75:963–980.

van Kesteren MT, Fernandez G, Norris DG, Hermans EJ (2010) Persistent schema-dependent hippocampal-neocortical connectivity during memory encoding and postencoding rest in humans. Proc Natl Acad Sci USA 107:7550–7555.

Wagner AD, Pare-Blagoev EJ, Clark J, Poldrack RA (2001) Recovering meaning: left prefrontal cortex guides controlled semantic retrieval. Neuron 31:329–338.

Wang MY, Wang J, Zhou J, Guan YG, Zhai F, Liu CQ, Xu FF, Han YX, Yan ZF, Luan GM (2017) Identification of the epileptogenic zone of temporal lobe epilepsy from stereo-electroencephalography signals: a phase transfer entropy and graph theory approach. Neuroimage Clin 16:184–195.

Watrous AJ, Tandon N, Conner CR, Pieters T, Ekstrom AD (2013) Frequency-specific network connectivity increases underlie accurate spatiotemporal memory retrieval. Nat Neurosci 16:349–356.

Yanagisawa T, Yamashita O, Hirata M, Kishima H, Saitoh Y, Goto T, Yoshimine T, Kamitani Y (2012) Regulation of motor representation by phase-amplitude coupling in the sensorimotor cortex. J Neurosci 32:15467–15475.

Zhou Y, Sheremet A, Qin Y, Kennedy JP, DiCola NM, Burke SN, Maurer AP (2019) Methodological considerations on the use of different spectral decomposition algorithms to study hippocampal rhythms. eNeuro 6: ENEURO.0142-19.2019.